

Dalton Transactions

Accepted Manuscript



This is an *Accepted Manuscript*, which has been through the Royal Society of Chemistry peer review process and has been accepted for publication.

Accepted Manuscripts are published online shortly after acceptance, before technical editing, formatting and proof reading. Using this free service, authors can make their results available to the community, in citable form, before we publish the edited article. We will replace this *Accepted Manuscript* with the edited and formatted *Advance Article* as soon as it is available.

You can find more information about *Accepted Manuscripts* in the [Information for Authors](#).

Please note that technical editing may introduce minor changes to the text and/or graphics, which may alter content. The journal's standard [Terms & Conditions](#) and the [Ethical guidelines](#) still apply. In no event shall the Royal Society of Chemistry be held responsible for any errors or omissions in this *Accepted Manuscript* or any consequences arising from the use of any information it contains.



www.rsc.org/dalton



Journal Name

ARTICLE

Bifluoride ($[\text{HF}_2]^-$) formation at the fluoridated aluminium hydroxide/water interface

Received 00th January 20xx,
Accepted 00th January 20xx

DOI: 10.1039/x0xx00000x

www.rsc.org/

Kenichi Shimizu^a, Gordon W. Driver^b, Marie Lucas^b, Tobias Sparrman^b, Andrey Shchukarev^b, Jean-François Boily^{*b}

This study uncovers bifluoride-type (difluorohydrogenate(I); $[\text{HF}_2]^-$) species formed at mineral/water interfaces. Bifluoride forms at $\equiv\text{Al-F}$ surface sites resulting from the partial fluoridation of gibbsite ($\gamma\text{-Al}(\text{OH})_3$) and bayerite ($\alpha\text{-Al}(\text{OH})_3$) particles exposed to aqueous solutions of 50 mM NaF. Fluoride removal from these solutions is proton-promoted and results in a strongly self-buffered suspensions at circumneutral pH, proceeds at a F:H consumption ratio of 2:1, and with recorded losses of up to 17 mM fluoride (58 F/nm²). These loadings exceed crystallographic site densities by a factor of 3-4, yet the reactions have no resolvable impact on particle size, shape and mineralogy. X-ray photoelectron spectroscopy (XPS) of frozen (-155 °C) wet mineral pastes revealed coexisting surface F and HF^0 species. Electron energy loss features pointed to multilayer distribution of these species at the mineral/water interface. XPS also uncovered a distinct form of Na^+ involved in binding fluoride-bearing species. XPS and solid state magic angle spinning ¹⁹F nuclear magnetic resonance measurements showed that these fluoride species were highly comparable to a sodium-bifluoride (NaHF_2) reference. First layer surface species are represented as $\equiv\text{Al-F-H-F-Al}\equiv$ and $\equiv\text{Al-F-Na-F-Al}\equiv$, and may form multi-layered species into the mineral/water interface. These results consequently point to a potentially overlooked inorganic fluorine species in a technologically relevant mineral/water interfacial systems.

Introduction

Inorganic chemical reactions involving aluminium-fluoride interactions are of high relevance to a variety of geochemical², environmental^{3, 4} as well as technological⁵⁻⁹ processes. Aluminium fluoride (AF) catalysts are of notable technological interest, and the chemistry of their related aluminium hydroxo fluoride (AHF)⁵⁻⁹ phases have received particular attention given their predispositions at forming in the presence of atmospheric and liquid water.

An intriguing development in this field of study pertains to the stabilization of the bifluoride anions (difluorohydrogenate(I), $[\text{HF}_2]^-$) at solid/gas interfaces. HCl and HF vapor binding to NaF(s) ¹¹ and $\beta\text{-AlF}_3(\text{s})$ surfaces^{12, 13} are prime examples of systems favouring bifluoride surface species. Theoretical work¹³ suggests that HF binding to undercoordinated $\equiv\text{Al}$ defect sites leads to a bifluoride complex of the type $\equiv\text{Al-F-H}\cdots\text{F-Al}\equiv$ via hydrogen bonding to a pre-existing neighboring $\equiv\text{Al-F}$ site. The occurrence of bifluoride species has, otherwise, not been extensively documented at other interfaces.

Resolution of interfacial bifluoride species can be especially important, specifically in terms of its strong Lewis character, weak Brønsted acidity ($K = [\text{HF}_2^-]/[\text{HF}][\text{F}] \approx 0.38$ in aqueous media¹⁵⁻¹⁷), and remarkably strong hydrogen bond.¹⁸⁻²⁰ Solids containing this anion (*e.g.* $[\text{NH}_4][\text{HF}_2]$) have been synthesized as early as 1856,²¹ later prepared as siliconium varieties of $[\text{HX}_2]^-$ salts (where X = Cl, Br and I) in 1903,²² and as higher order trihalodihydrogenate(I) polymers of the $[\text{H}_2\text{X}_3]^-$ type in 1909.²³ Formation of $[\text{H}_n\text{X}_{n+1}]^-$ species ($n = 1-6$), as well as mixed X anionic species, are furthermore one of the few examples of hydrogen(I) coordination chemistry²⁴ that occur solely as a function of a long lived, independent 3-centre 4-electron μ_2 -hydrogen-bond. This feature thus contrasts with other counterpart compounds whose transient entities merely provide a secondary structure (*e.g.* in liquid water¹⁷), or that persist only through stabilization of local environments in the solid-state (*e.g.* $[\text{H}(\text{NO}_3)_2]^-$ in various crystal structures^{25, 26}).

Given these remarkable properties, resolution of interfacial forms of bifluoride could be potentially impactful for predicting the reactivity of solid surfaces contacted with fluoride-rich fluids. Al-bearing solids are of particular interest given the strength of the Al-F bond. Previous extensive work on aluminium (oxy)hydroxide solids and their polyoxometallate counterparts^{27, 28} contacted with fluoride-bearing solutions resolved the nature of OH/F ligand exchanges^{10, 28, 29} which produce terminal H-F and bridging $\mu\text{-F}$ sites. Such surface bound fluoride has played an important role as a mineralizing agent in zeolite synthesis.³⁰⁻³²

^a Physical and Theoretical Chemistry Laboratory, University of Oxford, OX1 3QZ Oxford, United Kingdom

^b Department of Chemistry, Umeå University, SE-901 87 Umeå, Sweden

* corresponding author: jean-francois.boily@chem.umu.se

Electronic Supplementary Information (ESI) available: [details of any supplementary information available should be included here]. See DOI: 10.1039/x0xx00000x

In this study, we build upon these previous achievements by presenting new experimental evidence showing that aluminium hydroxide surfaces contacted with circumneutral pH solutions containing high levels of fluoride (*i.e.* 50 mM) favor hydrogen-bonded fluoride species, in the form of a networks of interconnected bifluoride species. This evidence is supported by cryogenic X-ray photoelectron spectroscopy (XPS), Nuclear Magnetic Resonance (NMR) and wet chemical work on gibbsite (γ -Al(OH₃)) and bayerite (α -Al(OH₃)) particles, two phases of considerable importance nature and industry.³³

Experimental section

Chemicals and materials

All chemicals were used as received and made in de-ionized water Milli-Q plus water. One 100 mM NaF stock solution was used throughout the experiment. Hydrofluoric and perchloric acids were diluted from concentrated sources, and standardized using Trizma base before use. Sodium hydroxide solutions were, in turn, prepared from NaOH pellets and standardized from the standardized acid titrants. Solid sodium difluorohydrogenate (Sigma-Aldrich), AlF₃ (Sigma-Aldrich), and a natural specimen of natural cryolite (Na₃[AlF₆]; mineral collection of Umeå University) were freshly ground or cleaved prior XPS analysis.

Nanosized gibbsite (α -Al(OH₃)) particles were synthesized according to Gastuche and Herbillon³⁴ by sequential addition of 1 M NaOH to a 1 M AlCl₃ aqueous solution of pH 4.6. Reactions were carried out in a solution mixed with a propeller in a polyethylene bottle and under an atmosphere of N₂(g). The resulting amorphous aluminium hydroxide suspension was then heated for 2 h at 40 °C and dialyzed in an oven at 60 °C. Dialysis water was changed on a daily basis until the resistivity of the dialysis water was comparable to that of Milli-Q water. Bayerite (β -Al(OH₃)) was produced by aging a γ -alumina (99.995% purity, Sumitomo Chemical Co., Ltd) aqueous suspension for 12 years. A portion of the suspensions was dried overnight at 50 °C in an oven and stored dry for characterization.

Powder X-ray diffraction (Bruker D8 Advance device working in θ - 2θ mode using Cu K α radiation) confirmed that gibbsite and bayerite were the sole crystallographic phases in the suspensions. Fourier transform infrared spectroscopy (FTIR; Bruker Vertex 70/v) confirmed this finding by retrieving the characteristic O-H stretching and bending modes of gibbsite and bayerite. Furthermore, XPS measurements (Section 2.3) produced values in agreement with literature values.^{35, 36} 90-point N₂(g) adsorption/desorption isotherms (Micrometric Flowsorb II 2300) returns a B.E.T. specific surface area of 41 m²/g for gibbsite and 67 m²/g for bayerite.

Titration and adsorption experiments

Aqueous suspensions of gibbsite or bayerite (4.5 g/L) in 50 mM NaF and NaClO₄ were prepared at least two days prior cryogenic XPS measurements. HF, HClO₄ or NaOH were added to 5 mL aliquots of the gibbsite suspension and mixed for 24 h under an atmosphere of water-saturated N₂(g). All acids and the base were standardized immediately prior to experiments by colorimetric titrations. The suspensions were thereafter centrifuged (4000 rpm for 15 min) and the supernatants separated to measure concentrations of unreacted fluoride ion and pH. A pH combination electrode and fluoride ion selective electrode (ISE) were calibrated

daily. A fluoride ion selective electrode was calibrated immediately prior to measurement using standard NaF solutions prepared from the same stock solution. Soluble aluminium in selected acidified supernatants was measured by inductively coupled plasma (ICP) analysis.

X-ray photoelectron spectroscopy

The centrifuged wet gibbsite pastes were smeared onto a molybdenum sample holder that was immediately loaded into the spectrometer air-lock chamber onto the pre-cooled (-170°C) claw of the sample transfer rod. This procedure froze the wet gibbsite paste within 10-15 s. After 45 s of cooling, the pressure in the chamber was lowered to 10⁻⁷ torr while maintaining the temperature. The sample was thereafter transferred to the analysis chamber for XPS analysis. All spectra were recorded at 10⁻⁹ torr and at -155°C using a Kratos Axis Ultra electron spectrometer equipped with a delay line detector (Manchester, UK). A monochromated Al K α source operated at 150 W, a hybrid lens system with a magnetic lens, providing an analysis area of 0.3 × 0.7 mm, and a charge neutraliser were used. Survey spectra were collected from 1100 to 0 eV at pass energy of 160 eV, and confirmed the absence of impurities other than typical atmospheric and instrumental carbon (Fig. S2a; Table S1). High-resolution spectra for Na 1s, F 1s, O 1s, C 1s, Cl 2p and Al 2p were collected at pass energy of 20 eV. All high-resolution XPS spectra were processed using Shirley backgrounds, and peaks were modeled using a 70% Gaussian/30% Lorentzian function, and referenced to the 285.0 eV line of aliphatic carbon.

Nuclear Magnetic Resonance

Solid state magic angle spinning ¹⁹F-NMR (SS-MAS ¹⁹F-NMR) was used to determine the fluorine speciation at the gibbsite surface. Typically between 50–100 mg of the material was packed into a 4 mm zirconium oxide rotor. All NMR experiments were performed on a Bruker Avance III 500 MHz spectrometer with a ¹⁹F operating frequency of 470.59 MHz. We used K⁷⁹Br to adjust the magic angle to 54.7°. Rotors packed with sample were spun at 14 kHz ± 3 Hz inside a 4 mm MAS-probe with a bearing air temperature of 288 K. Spectra were acquired using a 2.8 μ s ¹⁹F 90° excitation pulse, followed by a rotor synchronized Hahn echo and acquisition start after two full rotor periods. The spectral width of 530 ppm and relaxation delay of 60 s was used. A wet Na[HF₂] reference spectrum was collected using 16 scans whereas gibbsite spectra were collected using 800 scans. In order to clearly identify isotropic lines and spinning sidebands the corresponding spectra were also collected at 10 kHz spinning. A line broadening of 400 Hz was applied to all spectra. ¹⁹F chemical shifts are given relative to external NaF_(s) (at δ = -222.9 ppm) versus CFCl₃.

Results and Discussions

A suspension of 4.5 g/L ([Al]_{tot}=57 mM) gibbsite particles equilibrated in 50 mM NaF and reacted with up 10 mM HF or HClO₄ displayed a particularly strong buffering capacity in circumneutral pH region (Fig. S1). This buffering region contrasts sharply with typical mineral surface titrations (*e.g.* iron oxides) where more acidic pH values can be readily achieved by addition of moderate concentrations of acid (*e.g.* HCl, HClO₄) in relatively inert background electrolytes (*e.g.* NaCl, NaClO₄).^{37, 38} Soluble fluoride concentrations along this buffering region systematically decreased with each subsequent addition of HF or HClO₄ with a F/H consumption ratio close to 2:1 (Figs. 1, S2). As an example, addition of 10 mM HF to this system resulted in a fluoride loading of 46

fluoride/nm², a value that is ~3 times larger than the crystallographically available hydroxo population at gibbsite particle surfaces. At the same time, soluble levels of Al were in the 50-96 μ M range (Fig. S2), indicating that gibbsite dissolution is not as extensive in the time frame of these experiments, as would otherwise be predicted by thermodynamic predictions (Figs. S2 & S3).

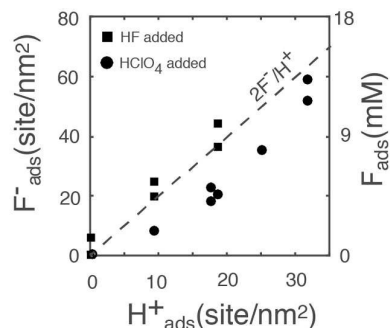


Figure 1. Fluoride loadings (F_{ads}) derived from ISE measurements (site/nm²; fluoride sorbed per specific surface area of gibbsite) as a function of adsorbed protons added as HF or HClO₄. Obtained from aqueous suspensions of gibbsite (4.5 g/L, 40.8 m²/g) at pH the 7.6-9.7 range. Soluble Al(III) were in the 50-96 μ M range.

Aqueous speciation calculations based on these measured Al concentrations suggest that aluminium-fluoride species represent no more than ~0.2 mM (0.4-0.6 %) of the original 50 mM fluoride in the system (Figs. S2 & S3). Measured fluoride losses by ISE cannot therefore be accounted by aqueous complexation. These results moreover show that protons consumed by dissolution represent an insignificant fraction of those involved in fluoride co-adsorption reactions. Thus, loss of fluoride from aqueous solutions is predominantly proton-promoted, irrespective of the source being HF or HClO₄, occurs in a narrow pH region (7.6-9.0) and is not associated with any extensive dissolution of gibbsite.

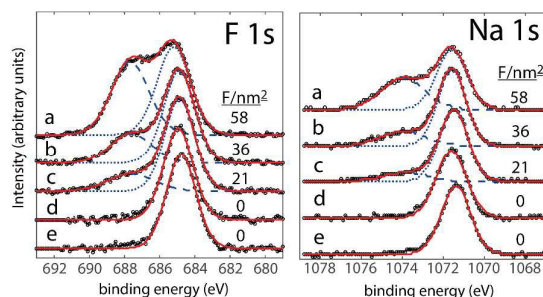


Figure 2. High resolution F 1s (left) and Na 1s (right) spectra of frozen (-155 °C) wet gibbsite particles reacted in NaF solutions at various HF (a=10.3, b=5.7, c=2.8, d=0.0 mM) and NaOH (e=0.4 mM) concentrations, and under a constant total ionic strength of 50 mM (Na)F. Fluoride loadings (F/nm^2) were derived from ISE measurements (Fig. 1). Blue dashed lines are component fits and red full lines total fits to experimental data.

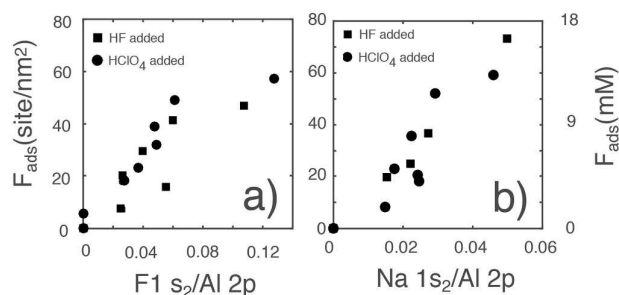


Figure 3. Fluoride loadings (F_{ads}) derived from ISE measurements (site/nm²; fluoride sorbed per specific surface area of gibbsite) as a function of the atomic percentage of (a) fluoride in the F 1s₂ peak at 687.6 eV and (b) sodium in the Na 1s₂ peak at 1073.5 eV. Atomic percentages were normalised for those of aluminium (Al 2p at 74.6 eV).

Cryogenic XPS analyses of the wet centrifuged gibbsite pastes provided more insight into the nature of adsorbed fluoride species (Figs. 2 & S4). All gibbsite samples considered for this work consistently retrieved a total Na:F_{ads} ratio of ~1:2 which, alongside the aforementioned F:H ratio of ~2:1 (Fig. 1), suggest an average compositional mixture of the type Na:F:H ~1:2:1 at the gibbsite/water interface. The F 1s photoelectron line of the wide spectra (Fig. S2a) of samples reacted along the pH-buffering region revealed an electron energy loss (EEL) peak at 700-760 eV, the area of which is proportional to fluoride loadings. The EEL is evidence for a multilayer distribution³⁹ of fluoride ions in the sample, and therefore one that can support evidence for the unusually large site densities derived by ISE measurements.

The high-resolution F 1s spectrum (Fig. 2a) features peaks at 685.0 (F 1s₁) and 687.6 eV (F 1s₂), the latter increasing in area with fluoride loading (Fig. 3a). This surface species is also accompanied by an additional feature Na 1s₂=1073.5 eV (Figs. 2b & 3b) and, just as in the total ratios, the Na 1s₂:F 1s₂ ratios are also ~1:2. We note that the 687.6 eV F species is only present when contacted water, as this peak and its associated EEL peak disappear concomitantly under (i) prolonged cryogenic conditions, where ice ultimately sublimates, and (ii) upon loss of water and HF(g), as seen through decreases in F/Na ratios during *in vacuo* warming of the samples to 25 °C. Finally, we also note that these results were not unique to the case of gibbsite. Highly comparable cryogenic F 1s and Na 1s XPS spectra were similarly obtained for bayerite (Fig. S5), a phase of identical chemical composition as gibbsite but of different crystallographic structure and surface termination³³. Our results ought therefore be generalised to other forms of aluminium hydroxide phases.

In order to identify the nature of the species formed at the gibbsite and bayerite surfaces we first considered the possibility for the formation of secondary phases. While thermodynamic calculations (using constants from the literature^{1, 10, 14}; cf Fig. 4) suggested that AlF₃(s), NaAl₂F₆(s) were unlikely to form, recently published solubility constants for the AlF₂OH(s) phase^{14, 40} matched the low soluble Al values measured from gibbsite suspensions, as shown in Fig. 4. Scanning Electron Microscope imaging (not shown) did not reveal any detectable changes in particle size or morphology that could suggest any considerable physical changes. The Al 2p XPS spectrum did not, neither reveal any extensive binding energy shifts (e.g. AlF₃(s) at 76.8 eV⁴¹, and AHF⁴¹ and Na₃[AlF₆] at 75.2 eV, Table S2) relative to pristine gibbsite (74.6 ± 0.1 eV). We consequently favour the concept that the gibbsite (sub)surface must have

undergone partial fluoridation reactions, thus producing a (partial) coating of the type $\text{AlF}_2\text{OH}(\text{s})$ and with surface complexes of the type $\equiv\text{Al-F}$, where $\equiv\text{Al}$ is a surface-bound aluminium (Fig. 5).⁴² Species of this type had been previously identified at AHF surfaces.⁴³ We thus ascribe the lower solubility of the particles (in relation to the predicted values) to passivation by fluoride, a situation much akin to the role that the fluoride plays in suppressing hydroxyapatite solubility.^{44,45}

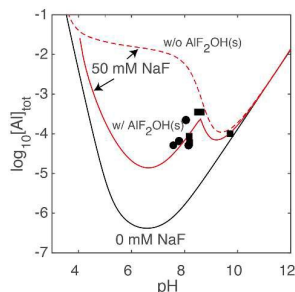


Figure 4. Gibbsite solubility in 0 and 50 mM NaF. Thermodynamic speciation calculations of the $\text{Al}(\text{III})\text{-F}(\text{I})\text{-H}_2\text{O}$ system (298 K, $I=0$) were carried out using equations and constants listed in Bodor *et al.*¹. Values for $\text{Na}_3\text{AlF}_6(\text{s})$ and $\text{AlF}_3(\text{s})$ solubility are taken from Nordin *et al.*¹⁰, and the one for $\text{AlF}_2(\text{OH})(\text{s})$ from Ntuk *et al.*¹⁴.

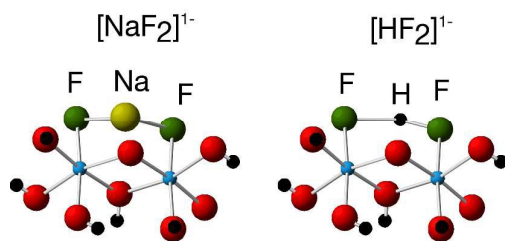


Figure 5. Schematic representation of $\equiv\text{Al-F}$ sites and their involvement in the stabilisation of $\equiv\text{Al-F-Na-F-Al}\equiv$ (left) and $\equiv\text{Al-F-H-F-Al}\equiv$ (right) surface species.

Acknowledging the presence of $\equiv\text{Al-F}$ sites at these fluoridated surfaces opens possibilities for explaining the singular attributes of the high energy F 1s and Na 1s peaks revealed by cryogenic XPS. We first note that the 687.6 eV peak could arise from both a Al-bound fluoride, as in $\text{AlF}_3(\text{s})$ ⁴¹, or by a HF-type (686.8 eV) species⁴⁶, as notably seen in fast-frozen droplets of HF solutions (Table S2). However, as changes were not seen in the Al 2p spectra from our proposed surface coating, it is unlikely that the F 1s spectra could display such a contrastingly stark response. As a result, we considered the possibility that HF-bearing species must be responsible for the high binding energy portion of the F 1s spectra, and that it was also strongly correlated to the high binding energy portion of the Na 1s spectra (Fig. 2b).

As detailed in the introduction, a species that accounts for a strong uptake of hydrogen-bonded HF at solid surfaces is the bifluoride anion. This possibility is certainly not unprecedented for AlF-type surfaces where HF(g) vapour binding can result in surface complexes of the type $\equiv\text{Al-F-H-F-Al}\equiv$, in which $\equiv\text{Al}$ is a surface-bound Al atom. By analogy, the $\equiv\text{Al-F}$ terminated surface provides

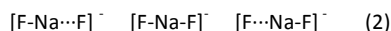
the environment required for the stabilization of bifluoride species from 50 mM NaF solutions.

In order to test this possibility we compared our XPS spectra of gibbsite and bayerite with those of a freshly cleaved sodium difluorohydrogenate(I) ($\text{Na}[\text{HF}_2]$) solid (Table S2; Figs. S5b & S6). Strong similarities in the narrow F 1s lines of the 685.0-688 eV region (Table S2) were particularly striking features that fully support the concept that bifluoride could be stabilised at these surfaces. Most notably, the full width at half maximum (3.4 eV) of $\text{Na}[\text{HF}_2]$ was strongly concordant with the high binding energy of the F 1s line of gibbsite and bayerite, and results from the resonance-like attributes of the bifluoride anion, here expressed as:



We note that these attributes are caused by large protic vibrations manifested as oscillations in the paramagnetic field with uniformity, akin to a pair of Helmholtz coils, and are produced by the negatively charged terminal fluoride ions.⁴⁷ Interestingly, the strength of those oscillations are not the same at the gibbsite and bayerite surfaces where the difference between high binding energy components in Na 1s and F 1s spectra (386.0 ± 0.2 eV, Table S1) are intermediate to those of between Na^+ and F^- (387.0 eV) and Na^+ and HF (385.6 eV) in NaHF_2 (Table S2). As the FH-F bond in $\text{Na}[\text{HF}_2]$ has a dissociation energy of 186 kJ/mole^{48, 49} and the H-F bond a value of 566 kJ/mole⁵⁰, the dissociation energy for bifluoride (*i.e.* F^- from HF_2^-) at the gibbsite surface could also lie between those of HF and F^- . Hydrogen bonding with surface hydroxo- and aquo-groups is consequently seen as contributing factor to the altered bond strength of these interfacial bifluoride species, and thus to the variations in binding energies seen in different samples under study.

Inspection of the Na 1s region reveals an additional factor concerning the nature of this interfacial bifluoride species. First, this region reveals no clear EEL features, and therefore suggests that sodium is mostly confined to a smaller number of adsorption layers than fluoride, a result consistent with the expectation of close interactions between this counterion and surface (hydr)oxo groups. The full width at half maximum of the Na 1s peak is however unusually large in comparison with that other mineral interfacial systems previously studied in our group by cryogenic XPS.⁵¹ This result suggests that the lifetimes of interfacial resonance structures are longer than the time necessary for photoionization ($\approx 10^{-16}$ sec), and can therefore effectively be explained by its interactions with a species like bifluoride. In fact, the resonance-like attributes of this species are represented as:



where sodium is a surface-bound species that is located in a narrow region of the interface.

Finally, as an additional independent means to validate bifluoride formation at AHF-coated aluminium hydroxide surfaces, we compared SS-MAS ^{19}F -NMR spectra of our freshly cleaved sodium difluorohydrogenate(I) ($\text{Na}[\text{HF}_2]$) solid with those of gibbsite and bayerite each reacted with 10 mM HF in 50 mM NaF (Fig. 6). The ^{19}F resonance of the $\text{Na}[\text{HF}_2]$ reference standard was observed at $\delta = -189$ ppm (spinning side bands were observed at repeating intervals of ~ 14 kHz about the central isotropic signal). Our

fluoride-reacted gibbsite samples gave rise to a predominant resonance at $\delta = -187$ ppm. This is in complete accord with that of the $[\text{HF}_2]^-$ anion observed with the reference standard ($\delta = -189$ ppm), especially considering the following: (1) an exact match between the ^{19}F chemical shift (δ/ppm) would be quite unexpected given differences in shielding at the gibbsite surface and the solid reference sample; (2) the frequency scale of these experiments; and (3) the full half width maxima of these signals. The NMR measurements therefore serve strongly as additional evidence of bifluoride formation at the minerals surfaces, in full support of the XPS data.

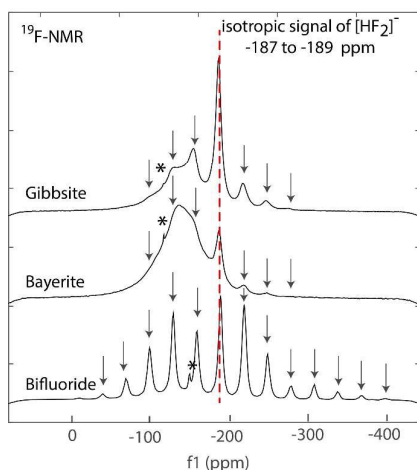


Figure 6. SS-MAS ^{19}F -NMR spectra recorded at ~ 20 °C for (top) wet gibbsite paste and (middle) wet bayerite paste both equilibrated with 10 mM HF in 50 mM NaF at pH 7.6. The reference spectrum of authentic wet $\text{Na}[\text{HF}_2]$ (bottom) is also shown for comparison ($n_s = 16$). Isotropic signals from the $[\text{HF}_2]^-$ anion are between $\delta = -187$ and -189 ppm in all three samples (relative to external $\text{NaF}_{(s)}$ versus CFCl_3). Spinning side bands are observed in repeating intervals of ~ 14 kHz from the central isotropic resonance of $[\text{HF}_2]^-$. Closer inspection of the spectra revealed minor isotropic resonances (marked in *), at $\delta = -150$ ppm in $\text{Na}[\text{HF}_2]$ and $\delta = -118$ ppm in gibbsite and bayerite, originating from $\text{NaF}_{(aq)}$ (spinning side-bands were not observed for this resonance which integrated to $\leq 1\%$). The broad resonance at $\delta = -139$ ppm appearing in the bayerite spectrum with $n_s = 1024$ (visible to a lesser extent in the gibbsite spectrum with $n_s = 800$) is a background signal due to per-fluorinated materials of the probe stator.

Conclusions

Fluoride is a strong complexing agent responsible for enhancing aluminum hydroxide solubility by means of OH/F exchange and formation of direct Al-F bonds in surface and aqueous complexes. When exposed to concentrated NaF aqueous media, aluminum hydroxide suspensions become strongly buffered systems due to a phase transformation which, for the time frame considered in this work, results in a partially fluoridated surface of the type $\text{AlF}_2\text{OH}(s)$ containing $\equiv\text{Al-F}$ surface complexes.

The creation of Al-F terminated surfaces provided a means for the stabilization of interfacial forms of bifluoride. Mechanisms include those outlined for the gas phase, resulting in first-layer species of the type $\equiv\text{Al-F-H-F-Al}\equiv$. Sodium is also strongly

coupled to this process, and could yield the analogous $\equiv\text{Al-F-Na-F-Al}\equiv$ species, but could also possibly host a bifluoride species in a configuration of the type $\equiv\text{Al-OH}\cdots\text{Na-FHF}$. These species may also extend into the mineral/water interface, thus accounting further for the multilayer distributions of fluoride species seen by XPS. Collectively, these results point to the formation of bifluoride at the gibbsite surface, a potentially overlooked inorganic fluorine species that could also occur at environmentally and technologically relevant interfaces.

Acknowledgements

This work was supported by a grant from the Swedish Research Council to JFB (2012-2976). The authors acknowledge the Umeå Core Facility Electron Microscopy (UCEM) and the Nuclear Magnetic Resonance (NMR) platforms of Chemical Biological Centre of Umeå University for access and support.

Notes and references

1. A. Bodor, I. Toth, I. Banyai, L. S. Zekany and S. Sjöberg, *Geochim. Cosmochim. Acta*, 2003, **67**, 2793-2803.
2. Y. M. Deng, D. K. Nordstrom and R. B. McCleskey, *Geochim. Cosmochim. Acta*, 2011, **75**, 4476-4489.
3. D. L. Ozsvath, *Rev. Environ. Sci. Biotechnol.*, 2009, **8**, 59-79.
4. S. Jagtap, M. K. Yenkie, N. Labhsetwar and S. Rayalus, *Chem. Rev.*, 2012, **112**, 2454-2466.
5. C. Rongeat, M. A. Reddy, R. Witter and M. Fichtner, *J. Phys. Chem. C*, 2013, **117**, 4943-4950.
6. L. P. Demyanova, V. S. Rimkevich and A. S. Buynovskiy, *J. Fluorine Chem.*, 2011, **132**, 1067-1071.
7. M. Nete, W. Purcell and J. T. Nel, *J. Fluorine Chem.*, 2014, **165**, 20-26.
8. W. Zhang, Z. Hu, Y. Liu, H. Chen, S. Gao and R. M. Gaschnig, *Anal Chem*, 2012, **84**, 10686-10693.
9. V. S. Rimkevich, A. A. Pushkin, I. V. Girenko and T. Y. Eranskaya, *Russian Journal of Non-Ferrous Metals*, 2014, **55**, 344-349.
10. J. P. Nordin, D. J. Sullivan, B. L. Phillips and W. H. Casey, *Geochim. Cosmochim. Acta*, 1999, **63**, 3513-3524.
11. R. S. C. Smart and N. Sheppard, *Proceedings of the Royal Society of London. A. Mathematical and Physical Sciences*, 1971, **320**, 417-436.
12. Y. Lee, J. W. DuMont, A. S. Cavanagh and S. M. George, *The Journal of Physical Chemistry C*, 2015, 150610114452004.
13. C. L. Bailey, A. Wander, S. Mukhopadhyay, B. G. Searle and N. M. Harrison, *Phys Chem Chem Phys*, 2008, **10**, 2918-2924.
14. U. Ntук, S. Tait, E. T. White and K. M. Steel, *Hydrometallurgy*, 2015, **155**, 79-87.

ARTICLE

Journal Name

- 15 15. C. B. Wooster, *JACS*, 1938, **60**, 1609-1613. 42
- 16 16. W. J. Hamer and Y. C. Wu, *Journal of Research of the National Bureau of Standards Section a-Physics and Chemistry*, 1970, **A 74**, 761-+. 43
- 17 17. D. G. Tuck, in *Progress in Inorganic Chemistry*, John Wiley & Sons, Inc., 1967, pp. 161-194. 44
- 18 18. J. Emsley, *Polyhedron*, 1985, **4**, 489-490. 45
- 19 19. A. M. Panich, *Chem. Phys.*, 1996, **196**, 511-519. 45
- 20 20. A. J. Sillanpää, C. Simon, M. L. Klein and K. Laasonen, *The Journal of Physical Chemistry B*, 2002, **106**, 11315-11322. 46
- 21 21. J. J. Berzelius, *Lehrbuch der Chemie*, Friedrich Vieweg und Sohn, Braunschweig, 1856. 47
- 22 22. W. Diltthey, *Berichte der deutschen chemischen Gesellschaft*, 1903, **36**, 923-930. 48
- 23 23. F. Kaufler and E. Kunz, *Ber. Dtsch. Chem. Ges.*, 1909, **42**, 2482-2487. 49
- 24 24. N. N. Greenwood and A. Earnshaw, *Chemistry of the Elements*, Butterworth-Heinemann, Oxford, 1997. 50
- 25 25. K. Garbett, R. D. Gillard and R. Ugo, *Journal of the Chemical Society A: Inorganic, Physical, Theoretical*, 1966, 1137-1139. 51
- 26 26. B. D. Faithful, R. D. Gillard, D. G. Tuck and R. Ugo, *Journal of the Chemical Society A: Inorganic, Physical, Theoretical*, 1966, 1185-1188. 52
- 27 27. L. Allouche and F. Taulelle, *Chem. Commun.*, 2003, 2084.
- 28 28. W. H. Casey, *Chem. Rev.*, 2006, **106**, 1-15.
- 29 29. S. G. Cochiara and B. L. Phillips, *Clays Clay Miner.*, 2008, **56**, 90-99.
- 30 30. Y. Kalvachev, M. Jaber, V. Mavrodinova, L. Dimitrov, D. Nihtianova and V. Valtchev, *Microporous Mesoporous Mater.*, 2013, **177**, 127-134.
- 31 31. L. A. Villaescusa, P. S. Wheatley, I. Bull, P. Lightfoot and R. E. Morris, *JACS*, 2001, **123**, 8797-8805.
- 32 32. M. A. Camblor, A. Corma and S. Valencia, *J. Mater. Chem.*, 1998, **8**, 2137-2145.
- 33 33. G. Sposito, *The Environmental Chemistry of Aluminum*, CRC Press, 1995.
- 34 34. L. F. Harrington, E. M. Cooper and D. Vasudevan, *J. Colloid Interface Sci.*, 2003, **267**, 302-313.
- 35 35. T. Tsuchida and H. Takahashi, *J. Mater. Res.*, 1994, **9**, 2919-2924.
- 36 36. J. T. Klopogge, L. V. Duong, B. J. Wood and R. L. Frost, *J. Colloid Interface Sci.*, 2006, **296**, 572-576.
- 37 37. J. Rosenqvist, P. Persson and S. Sjöberg, *Langmuir*, 2002, **18**, 4598-4604.
- 38 38. T. Hiemstra, H. Yong and W. H. Van Riemsdijk, *Langmuir*, 1999, **15**, 5942-5955.
- 39 39. A. Shchukarev, J. F. Boily and A. R. Felmy, *J. Phys. Chem. C*, 2007, **111**, 18307-18316.
- 40 40. D. F. Lisbona, C. Somerfield and K. M. Steel, *Ind Eng Chem Res*, 2012, **51**, 12712-12722.
- 41 41. A. Makarowicz, C. L. Bailey, N. Weiher, E. Kemnitz, S. L. M. Schroeder, S. Mukhopadhyay, A. Wander, B. G. Searle and N. M. Harrison, *PCCP*, 2009, **11**, 5664-5673.
- 42 42. W. Kleist, C. Haessner, O. Storcheva and K. Kohler, *Inorg. Chim. Acta*, 2006, **359**, 4851-4854.
- 43 43. G. Scholz, S. Brehme, R. König, D. Heidemann and E. Kemnitz, *J. Phys. Chem. C*, 2010, **114**, 10535-10543.
- 44 44. A. Bengtsson, A. Shchukarev, P. Persson and S. Sjöberg, *Geochim. Cosmochim. Acta*, 2009, **73**, 257-267.
- 45 45. A. Bengtsson, A. Shchukarev, P. Persson and S. Sjöberg, *Langmuir*, 2009, **25**, 2355-2362.
- 46 46. K. Shimizu, A. Shchukarev, P. A. Kozin and J. F. Boily, *Langmuir*, 2013, **29**, 2623-2630.
- 47 47. F. Y. Fujiwara and J. S. Martin, *J. Chem. Phys.*, 1972, **56**, 4098-4102.
- 48 48. P. G. Wenthold and R. R. Squires, *J. Phys. Chem.*, 1995, **99**, 2002-2005.
- 49 49. S. Hirata, K. Yagi, S. A. Perera, S. Yamazaki and K. Hirao, *J. Chem. Phys.*, 2008, **128**.
- 50 50. D. B. d. B., *Nat. Stand. Ref. Ser. Nat. Bur. Stand.*, 1970, **60**, 1609-1613.
- 51 51. K. Shimizu, A. Shchukarev, P. A. Kozin and J. F. Boily, *Surface Science*, 2012, **606**, 1005-1009.